Proc. Natl. Acad. Sci. USA
Vol. 85, pp. 2393–2397, April 1988
Neurobiology

Channel protein engineering: Synthetic 22-mer peptide from the primary structure of the voltage-sensitive sodium channel forms ionic channels in lipid bilayers

(excitable membranes/ionic selectivity/protein structure/planar bilayers/single channels)

SHIGETOSHI OIKI*, WALEED DANHO†, AND MAURICIO MONTAL*‡

*Department of Neurosciences, Roche Institute of Molecular Biology, and †Peptide Research Department, Roche Research Center, Nutley, NJ 07110

Communicated by Gregorio Weber, December 1, 1987

ABSTRACT **A synthetic 22-mer peptide that mimics the sequence of a putative pore segment of the voltage-dependent sodium channel forms transmembrane ionic channels in lipid bilayers. Several features of the authentic sodium channel are exhibited by the synthetic peptide: (*i*) The single channel conductance of the most frequent event is 20 pS in 0.5 M NaCl. (*ii*) The single channel open and closed lifetimes are in the ms time range. (*iii*) The synthetic channel discriminates cations over anions but is nonselective between Na^+ and K^+. However, the synthetic channel displays no significant voltage dependence. Energetic considerations suggest a bundle of four parallel amphipathic α-helices as the most plausible channel structure. The synthetic 22-mer channel-forming peptide allows study of the mechanisms of ion permeation through sodium channels by protein engineering techniques.**

The sodium channel is the molecular entity responsible for the rising phase of the action potential in excitable cells (ref. 1; for review see ref. 2). Sodium channels sense the transmembrane electric field and respond by opening a transmembrane ionic channel with specificity for Na^+. The sodium channel protein was purified from several excitable tissues and its major component is a glycoprotein with an apparent M_r of ≈260,000 (3–6). Purified sodium channel proteins reconstituted in planar lipid bilayers show the same voltage dependence, neurotoxin sensitivity, and ionic specificity associated with native sodium channels in excitable cells (7–10). The genes encoding sodium channels from *Electrophorus electricus* (11), rat brain (12), and *Drosophila* (13) were cloned, and the cDNAs encoding the 260-kDa protein were sequenced. Furthermore, mRNA generated by transcription of the cloned cDNA encoding the rat brain sodium channel II when microinjected into *Xenopus* oocytes led to the expression of voltage-dependent sodium currents (14).

Given the primary structure of the sodium channel proteins, several models for the folding of the polypeptide chain across the bilayer membrane were suggested (11–13, 15–17). Our model (15) consists of four homologous regions, each containing eight membrane-spanning helical segments. The tertiary structure is pseudoradially symmetric. At its center four amphipathic transmembrane helices (18) meet with the hydrophilic surfaces facing inward to form a putative ion channel. The polar face of the amphipathic helices contains excess acidic residues, postulated to form the channel-lining structure in a cation-selective channel protein.

Several experimental approaches are currently in use to test the models. Notable among them is site-directed mutagenesis of functionally significant groups followed by expression of the mutated protein in the *Xenopus* oocyte system for subsequent electrophysiological characterization (19, 20). Here, we propose an approach with synthetic peptides to establish structure–function relationships in channel proteins. To locate the ion channel-forming domain, four peptides, 22 amino acids long, encompassing the sequences of the putative amphipathic helices of each of the four homologous repeats, were synthesized by solid-phase peptide synthesis (21). The ability of the peptides to form transmembrane ion channels was assayed by incorporating the pure synthetic putative channel peptide into lipid bilayers (22). We report here results obtained with one peptide, identified as Sc_1, that corresponds to one of the amphipathic segments postulated to form the sodium channel lining (15). Such segments (Fig. 1) show high homology in the four repeats as well as among electric eel (11), rat brain (12), and *Drosophila* (13). A detailed characterization of the conduction and gating properties of the synthetic ion channel-forming peptide is presented. Results lead us to suggest a general approach to study the mechanisms of ion permeation through membrane channel proteins by protein engineering; a preliminary account of this research was presented elsewhere (23).

MATERIALS AND METHODS

Materials. 1,2-Diphytanoyl-*sn*-glycero(3)phosphocholine was obtained from Avanti Biochemicals. All other chemicals were of the highest purity available commercially.

Synthesis of Peptides. The peptides were synthesized by solid-phase methods (21). Deprotection and cleavage from the resin were achieved by treatment with anhydrous HF according to the procedure of Tam *et al.* (24). The peptides were purified by reversed-phase HPLC on an 0.9 × 30 cm Waters μBondapak C_{18} column, using a linear gradient of acetonitrile in 0.1 M ammonium bicarbonate, pH 7.0. Purity of the peptides was confirmed by analytical HPLC, amino acid analysis, and microsequencing.

Peptide Incorporation into Planar Lipid Bilayers. The purified synthetic peptide was dissolved in chloroform/methanol (1:1) at a final concentration of 25 μM. 1,2-Diphytanoyl-*sn*-glycero(3)phosphocholine was dissolved in 1-hexane (Aldrich) to a final concentration of 2 mg/ml. The peptide solution was mixed with the lipid solution to achieve final peptide/lipid molar ratios in the range of 1/100–1/10,000.

The peptide/lipid solution in hexane was spread into monolayers at an air/water interface. The aqueous subphase was composed of 0.5 M NaCl or 0.5 M KCl buffered with 5 mM Hepes, pH 7.2. Bilayers were formed by the apposition

The publication costs of this article were defrayed in part by page charge payment. This article must therefore be hereby marked "*advertisement*" in accordance with 18 U.S.C. §1734 solely to indicate this fact.

Abbreviations: Sc_1, peptide corresponding to one of the amphipathic segments postulated to form the sodium channel lining; γ, single channel conductance; μ_H, hydrophobic moment; V, applied voltage; τ_o, open channel lifetime; τ_c, closed channel lifetime.

‡To whom correspondence should be addressed at his permanent affiliation: Departments of Biology and Physics, University of California at San Diego, La Jolla, CA 92093-0319.

	Sc_I																			
RAT BRAIN I	D	P	W	N	W	L	D	F	T	V	I	T	F	A	Y	V	T	E	F	V	D	L
RAT BRAIN II	N	P	W	N	W	L	D	F	T	V	I	T	F	A	Y	V	T	E	F	V	N	L
FLY	N	P	W	N	W	L	D	F	V	V	I	T	M	R	Y	A	T	I	G	M	E	V
EEL	D	P	W	N	W	L	D	F	S	V	V	T	M	T	Y	I	T	E	F	I	D	L

FIG. 1. Amino acid sequences of segments postulated to be involved in channel lining. The assigned channel segments for the rat brain I, rat brain II, *Drosophila* and *Electrophorus electricus* sodium channels corresponding to repeat I, referred to as Sc_1 (15), are illustrated. Note the high degree of conservation. The synthetic channel peptide corresponds to rat brain I Sc_1. Standard one-letter amino acid code is used.

of two monolayers at the tip of patch pipettes (22, 25). The pipettes were fabricated from either flint glass (Blue Tip, Lancer, St. Louis) or from Corning Glass 8161 (Garner Glass, Claremont, CA). EDTA (5 mM) was added to all solutions to chelate free lead or other divalent cations known to leach from the lead-containing glass (Corning 8161) (26). Planar bilayer experiments were done at 24 ± 2°C.

Electrical Recordings and Data Processing. All procedures were conducted as described previously in detail (25, 27, 28), with the following exceptions. Membrane current was stored in a video cassette recorder (Sony Betamax) equipped with a digital audio processor (Sony PCM 501 ES) modified according to Bezanilla (29) and commercially available from Unitrade (Philadelphia). The records were filtered at 3 kHz, unless otherwise indicated, with an 8-pole Bessel filter (Frequency Devices, Haverhill, MA) and digitized at 100 μs per point using an INDEC L-11/73-70 microcomputer system (INDEC, Sunnyvale, CA). This study contains results collected from >100 different membranes. The number of events analyzed to obtain each conductance and lifetime value was >200 and is reported as mean ± SEM. Total number of events analyzed was >50,000.

EXPERIMENTAL RESULTS

Structural Features of a Synthetic Peptide Predicted to Form the Sodium Channel Lining. Fig. 1 is a linear represen-

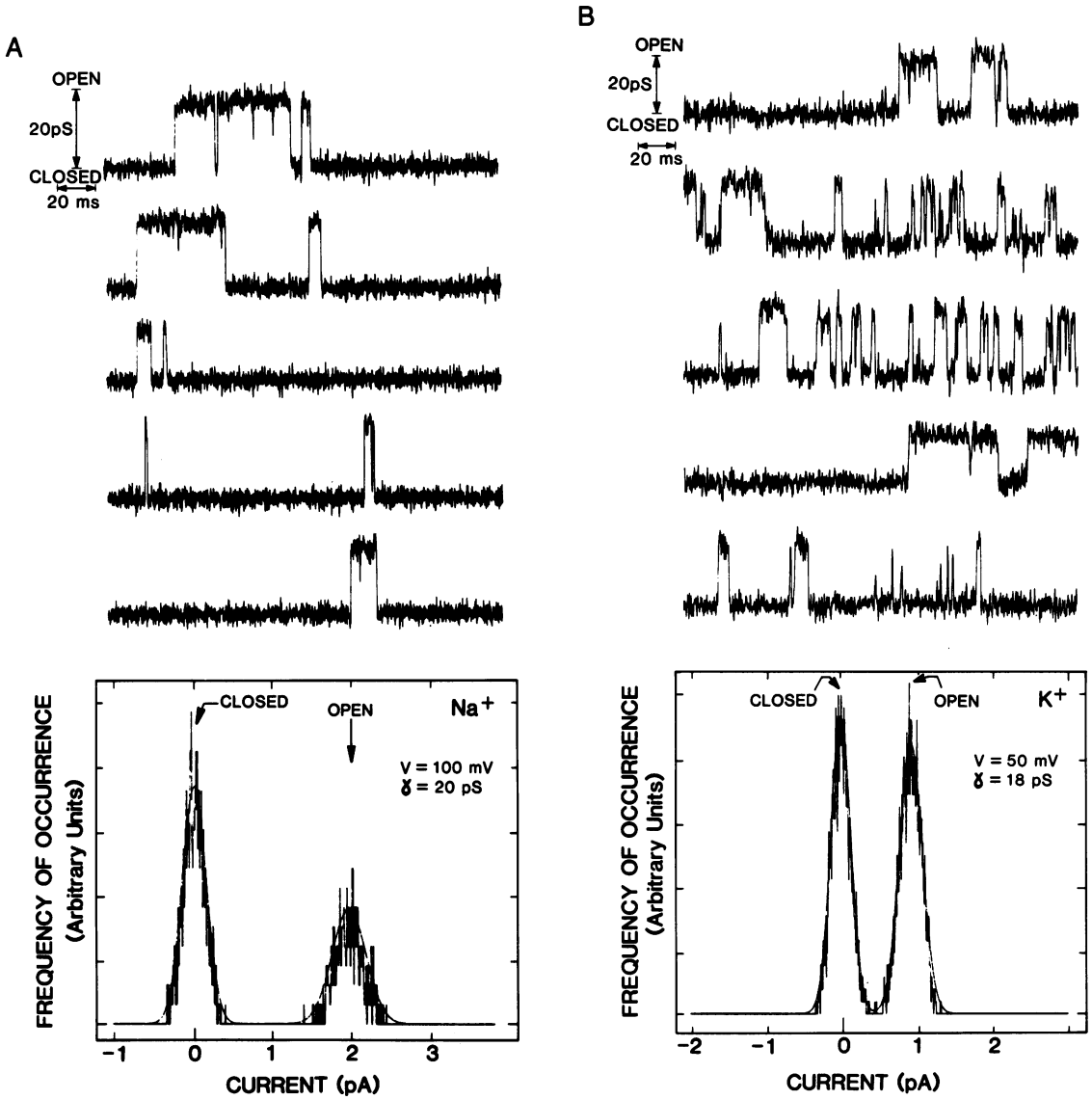

FIG. 2. Channel formation by the synthetic 22-mer peptide. Single-channel current records in 1,2-diphytanoyl-*sn*-glycero(3)phosphocholine membranes containing the synthetic channel peptide. (*A*) Single-channel records at V = 100 mV in symmetric 0.5 M NaCl/5 mM EDTA buffered with 5 mM Hepes, pH 7.2; bilayer resistance was 100 GΩ. (*B*) Single-channel records at V = 50 mV in symmetric 0.5 M KCl/5 mM EDTA buffered with 5 mM Hepes, pH 7.2. The bilayer resistance was 20 GΩ. Lower panels in *A* and *B* are the corresponding single-channel current histograms. The fitted Gaussian distributions (smooth curves) correspond to the channel closed state (peak at 0 current) and the open state (peaks at 2 pA and 0.9 pA for Na^+ and K^+, respectively). At the indicated V, γ = 20 pS for Na^+ and γ = 18 pS for K^+.

tation of the amino acid sequence of the synthetic peptide characterized in this paper. Secondary structure predictors (15, 30–32) suggest that such a sequence would form an amphipathic α-helix. Helical net and helical wheel representations suggest the segregation of lipophilic and hydrophilic residues on opposite faces of the helical cylinder with the two charges Asp-7 (D7) and Glu-18 (E18) in a linear array. Because spacing between residues is 1.5 Å in an α-helix, such a segment would be ≈33 Å long, a length sufficient to traverse the hydrocarbon core of the lipid bilayer (33).

The structure of the monomeric peptide would not locate it within the hydrophobic interior of the lipid bilayer due to its low hydrophobicity (34). However, a tetrameric array of four amphipathic transmembrane helices meeting with their polar surfaces facing inward could form the putative ion channel structure (Fig. 5). The hydrophobic moment, μ_H, is a measure of the amphiphilicity of the peptide perpendicular to the helical axis (34). For Sc_1, μ_H points toward the lipophilic surface of the array, whereas Asp-7 (D7) and Glu-18 (E18) are directed toward the polar interior. This quantitation supports the plausibility of an oligomeric structure for the peptide within the lipid bilayer.

Channel Formation by a Synthetic Amphipathic 22-mer Peptide Predicted to Form the Sodium Channel Lining. *Ionic conduction.* Currents flowing through individual synthetic channels recorded at V = 100 mV in symmetric 0.5 M NaCl (Fig. 2*A*) and in symmetric 0.5 M KCl (Fig. 2*B*) are illustrated. γ, measured from the amplitude of the single channel currents at the indicated V, is in the range of 14–26 pS for NaCl and 18–24 pS for KCl. These values of γ are for the most frequent events.

Ionic selectivity. The similarity of the single-channel current amplitudes in Na^+ and K^+ reflects the absence of selectivity of the channel between these two cations. This is confirmed by measurements of the current–voltage relationship in membranes containing several channels under bi-ionic conditions (Fig. 3). One of the aqueous compartments separated by the bilayer contains 0.45 M NaCl and 0.05 M KCl, whereas the other contains 0.45 M KCl and 0.05 M NaCl. The figure shows membrane current in response to a continuously cycled voltage from −100 mV to + 100 mV; the record indicates the presence of two channels in the membrane that undergo frequent open–closed transitions during both negative and positive branches of the cycle. The zero value of the current at V = 0 mV indicates lack of selectivity between Na^+ and K^+ (i.e., the reversal potential equals zero under bi-ionic conditions). The bilayer conductance, calculated from the slope of the line passing through the lowest current level, is 100 pS; from the line passing through the highest current level calculated bilayer conductance is 140 pS. The difference of 40 pS is accounted for by the two open channels detectable throughout the record with γ = 20 pS. Reversal potential measurements under single salt gradients of either NaCl or KCl indicate that the transference number for cations is >0.80. It is clear, therefore, that the synthetic peptide forms cationic channels across the bilayers which, however, lack selectivity between Na^+ and K^+.

Channel Gating Kinetics. In the description that follows, we focus on the most frequent conductance event—that exhibiting a γ = 20 pS. Quantitative analysis of the relative residence time of the channel in either closed or open states was determined from conductance histograms of long current records, such as those shown in Fig. 2, in which only one channel was open at any given time. The conductance histogram (*Lower*) is well fitted by the sum of two Gaussian distributions, one for the closed state and another for the open state. The relative frequency of occurrence of each state is determined from the area under the Gaussian distribution curve; the probability of the channel open state is ≈25% for Na^+ and ≈50% for K^+. The fraction of time that the channel spends in the open state is not significantly affected by the applied voltage (−100 mV < V < 100 mV) (Figs. 3 and 4*A*). Histograms of dwell times in open and closed states in symmetric 0.5 M NaCl are best fitted by one exponential. This indicates the occurrence of at least one open state and one closed state. The time constant for this open state is 1.27 ms and for the closed state is 1.44 ms (see Table 1).

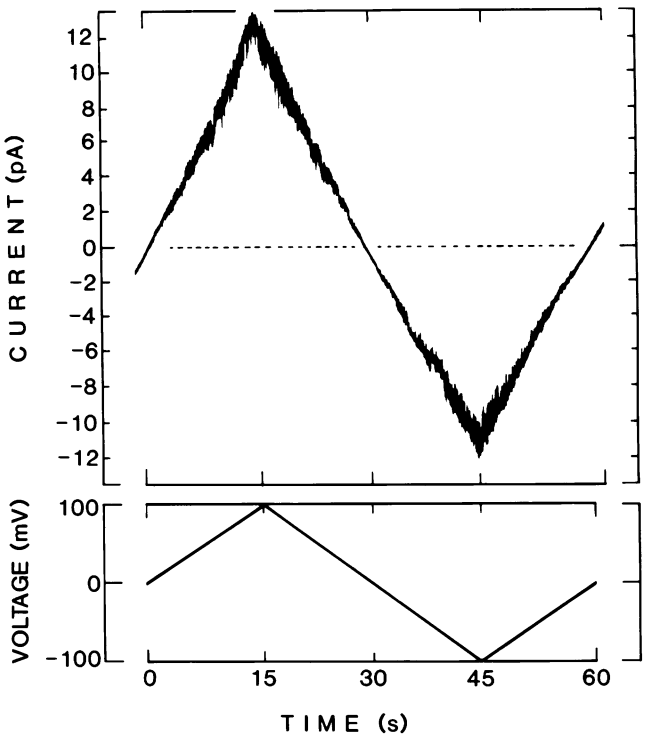

FIG. 3. Synthetic channel peptide is nonselective between Na^+ and K^+. Current records in response to a continuously cycled voltage from −100 mV to 100 mV under bi-ionic conditions. Membranes were formed from a peptide/1,2-diphytanoyl-*sn*-glycero(3)-phosphocholine solution in hexane at a 1/300 ratio. The aqueous compartments contained 5 mM EDTA/5 mM Hepes, pH 7.2. Bath solution was 0.45 M NaCl/0.05 M KCl; solution inside the patch pipette was 0.45 M KCl/0.05 M NaCl. The bilayer contained two channels with γ = 20 pS. Note that the current and voltage intersect at zero (3 instances), indicating that the reversal potential is zero. Signals were low-pass filtered at 200 Hz; bilayer resistance was 10 GΩ.

Distribution of Single-Channel Conductances Is Heterogeneous. A distinct feature of the single-channel recordings of

Table 1. Relative frequency of occurrence of distinct conductances and corresponding channel open and closed lifetimes in NaCl

γ, pS	Relative frequency of occurrence, %	τ_o, ms	τ_c, ms	*N*
5 < γ < 15	26	5.37 ± 1.72	7.09 ± 3.39	9
15 < γ < 25	36	1.27 ± 0.29	1.44 ± 0.40	17
25 < γ < 35	17	1.51 ± 0.95	2.08 ± 0.75	7
γ > 35	21	2.19 ± 0.76	0.61 ± 0.10	7

Membranes were formed in symmetric 0.5M NaCl solutions. γ was calculated from the Gaussian fits to conductance histograms (Fig. 2), and τ_o and τ_c were calculated from the exponential fits to probability density functions (25, 27, 28). Data were filtered at 2 kHz and were well fitted by a single exponential function. Due to limited time resolution of the system, the contribution of brief durations (<300 μs) was systematically disregarded. The table summarizes data collected from 81 membranes; total number of events analyzed was 14,280. Data are expressed as mean ± SEM; *N*, number of experiments. Other conditions were as for Fig. 2.

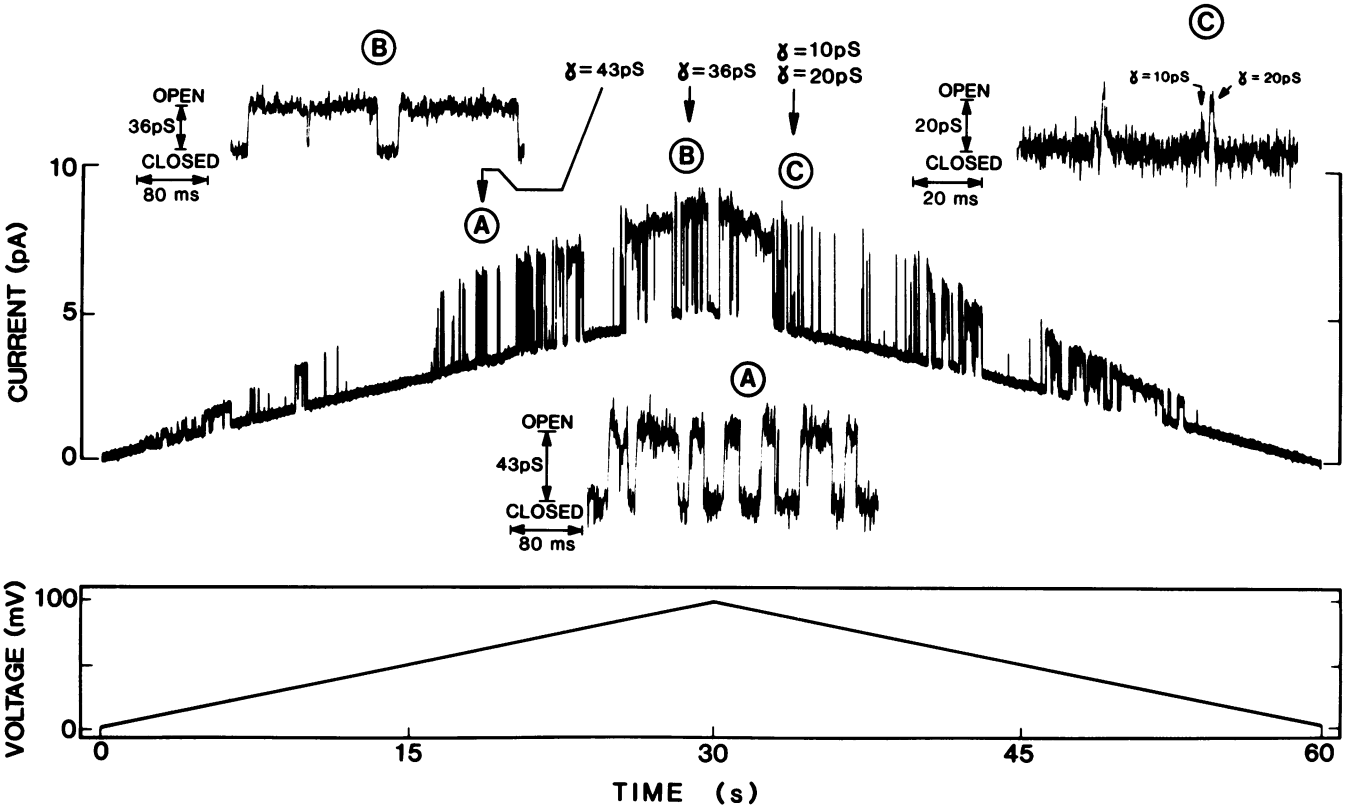

FIG. 4. Synthetic channel peptide conductance is heterogeneous. Current records in response to a continuously cycled voltage from 0 to 100 mV in symmetric 0.5 M NaCl/5 mM EDTA/5 mM Hepes, pH 7.2. The signal was low-pass filtered at 200 Hz. Sections indicated by the arrows (*A*, *B*, and *C*) and filtered at 3 kHz are displayed at high resolution (note the change in conductance and time calibrations); bilayer resistance was 20 GΩ.

the synthetic-channel peptide is the occurrence of openings with distinct amplitudes and variable open and closed lifetimes (Fig. 4). Several conductances, as calculated from the slopes of the lines, are resolved: $\gamma \simeq 8$ pS, $\gamma = 20$ pS, $\gamma = 36$ pS, and $\gamma = 43$ pS. The lowest-conductance events detected are in the range of 5–10 pS. The frequency of occurrence of this event may be underestimated on account of signal-to-noise ratio. The largest conductance events are in the range of 50–60 pS. Thus, γ exhibits a discrete distribution (Table 1). The lifetimes span the range from 0.6 ms to 19 ms. Overall, the most frequent event has a $\gamma \simeq 20$ pS (traces of Fig. 2*A*). Events with $\gamma > 35$ pS are significantly less frequent. They usually appear in brief bursts of openings, where $\tau_o < 1$ ms. In KCl, the most frequent event is also one with a γ in the range of 18–24 pS (traces of Fig. 2*B*). There is no apparent correlation between peptide/lipid ratio in the membrane-forming solution and the occurrence of a predominant conductance event.

DISCUSSION

The amphipathic 22-mer peptide, predicted from the amino acid sequence of the voltage-dependent sodium channel to be involved in channel lining, indeed forms cation-selective channels in lipid bilayers. Further, the sequence suggests that the central pore is assembled by the contribution of one channel segment from each of the four repeating units. We turn now to consider possible structures underlying the measured channels.

Energetic Considerations Suggest a Bundle of Four Amphipathic α-Helices as the Most Plausible Channel Structure. We investigated low-energy arrangements of α-helical bundles using the semi-empirical potential energy functions and optimization routines of the CHARMM program package (35). Locating the polar residues at the interior of the assembly and the apolar residues along the exterior surface, energy minimization was performed for helical bundles as a whole with no symmetry constraints and for bundles constructed through symmetry operations on a single peptide chain in a helical conformation. The three structures considered, with the symmetry used in parentheses, were as follows: a parallel trimer (C_3), a parallel tetramer (C_4), and an antiparallel tetramer (D_2). After the initial minimization, structures were further refined using molecular dynamics and reminimization. A detailed presentation of this analysis will appear elsewhere (V. Madison, S.O., W.D., M.M., unpublished data). We focus here on the structure of the channel lining generated by the parallel tetramer. Fig. 5 shows a computer-generated molecular model of the pore-forming structure produced by a bundle of four parallel α-helices. The optimized structure maintains the segregation of polar and nonpolar residues of the original model. Note that the pore is lined by two clusters of acidic groups—Asp-7s (D7s) and Glu-18s (E18s)—and the pore size is comparable to that inferred for the sodium channel protein. The antiparallel tetramer also has a similar central pore. In contrast, the parallel trimer appears as a close-packed occluded structure, without a patent polar pore (data not shown). The variety of conducting species inferred from the conductance measurements in the bilayers (Fig. 4) may correspond to various tetrameric arrays or larger oligomers of the peptide. Thus, our analysis suggests that a tetramer of the synthetic peptide adopts a structure reasonably suited to form the sodium channel lining.

Comparison of the Sodium Channel Protein and the Synthetic Channel Peptide. Ion conduction through open sodium channels and synthetic channels appears to proceed via similar diffusion pathways as inferred from similar values of γ in

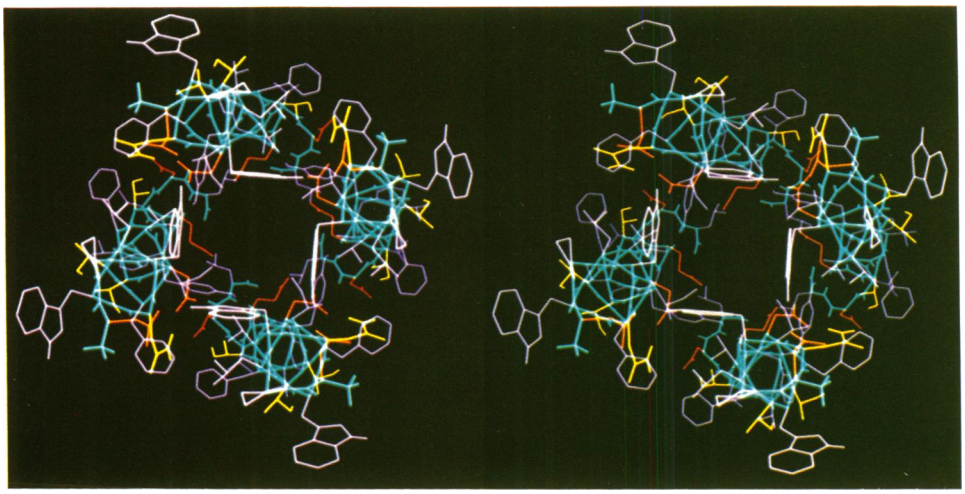

FIG. 5. A bundle of four amphipathic α-helices is a plausible structure for the synthetic channel peptide. Stereoviews of a computer-generated molecular model of the pore-forming structure (see text). Orthographic projection of the assembly (N-terminal view) showing the α-carbon backbone of the four helices (light blue), the acidic (red), basic (blue), polar-neutral (yellow), and lipophilic (purple) residues. Dimension of the central pore is 4 Å × 4 Å.

0.5 M NaCl (25 pS versus 20 pS). Authentic sodium channels exhibit a high permeability to Na^+ and Li^+ relative to other monovalent cations. The synthetic channel is cation selective but shows no intra-cation selectivity. Na^+/K^+ discrimination may arise in a heterotetramer conformed of four distinct amphipathic helices corresponding to the specific sequences of the four-repeats. The authentic sodium channel is exquisitely sensitive to applied voltage: channel opening is voltage dependent and favored by depolarization. The synthetic channel peptide undergoes open–closed transitions in the ms time range similar to the authentic protein. In contrast, these display no significant voltage dependence and proceed in the absence of an additional voltage-sensor component, as an inherent property of the synthetic structure.

Channel Protein Engineering as an Approach to Investigate Structure–Function Relationships in Channel Proteins. This report is a first step in the application of protein engineering to study channel proteins. In the absence of the exact x-ray structure of channel proteins, the strategy of using empirical secondary-structure predictions to postulate a structural model followed by the design and synthesis of peptides proposed to be transmembrane components of the assembly and the assay of the membrane action of such peptides in lipid bilayers appears to be, in principle, valuable. A salient advantage is that, by chemical synthesis, a given amino acid thought to be crucial for function can be substituted. The assay of the "analogue" will establish if such residue is functionally significant. The general validity of this strategy to other channels and receptors of known sequence can also be explored.

The valuable collaborations of T. Gabriel and V. Madison are gratefully acknowledged. We thank R. Horn, F. Gambale, and all the members of the Montal laboratory for valuable suggestions.

1. Hodgkin, A. L. & Huxley, A. F. (1952) *J. Physiol. (London)* **117,** 500–544.
2. Hille, B. (1984) *Ionic Channels of Excitable Membranes* (Sinauer, Sunderland, MA).
3. Agnew, W. S., Levinson, S. R., Brabson, J. S. & Raftery, M. A. (1978) *Proc. Natl. Acad. Sci. USA* **75,** 2606–2610.
4. Barchi, R. L., Cohen, S. A. & Murphy, L. E. (1980) *Proc. Natl. Acad. Sci. USA* **77,** 1306–1310.
5. Hartshorne, R. P. & Catterall, W. A. (1981) *Proc. Natl. Acad. Sci. USA* **78,** 4620–4624.
6. Lombet, A. & Lazdunski, M. (1984) *Eur. J. Biochem.* **141,** 651–666.
7. Hartshorne, R. P., Tamkun, M. & Montal, M. (1986) in *Ion Channel Reconstitution,* ed. Miller, C. (Plenum, New York), pp. 337–362.
8. Levinson, S. R., Duch, D. S., Urban, B. W. & Recio-Pinto, E. (1986) *Ann. N.Y. Acad. Sci.* **479,** 162–178.
9. Agnew, W. S., Rosenberg, R. L. & Tomiko, S. A. (1986) in *Ion Channel Reconstitution,* ed. Miller, C. (Plenum, New York), pp. 307–335.
10. Tanaka, J. C., Furman, R. E. & Barchi, R. L. (1986) in *Ion Channel Reconstitution,* ed. Miller, C. (Plenum, New York), pp. 277–305.
11. Noda, M., Shimizu, S., Tanabe, T., Takai, T., Kayano, T., Ikeda, T., Takahashi, H., Nakayama, H., Kanaoka, Y., Minamino, N., Kangawa, K., Matsuo, H., Raftery, M. A., Hirose, T., Notake, M., Inayama, S., Hayashida, H., Miyata, T. & Numa, S. (1984) *Nature (London)* **312,** 121–127.
12. Noda, M., Ikeda, T., Kayano, T., Suzuki, H., Takeshima, H., Kurasaki, M., Takahashi, H. & Numa, S. (1986) *Nature (London)* **320,** 188–192.
13. Salkoff, L., Butler, A., Wei, A., Scavarda, N., Giffen, V., Ifune, C., Goodman, R. & Mandel, G. (1987) *Science* **237,** 744–749.
14. Stühmer, W., Methfessel, C., Sakmann, B., Noda, M. & Numa, S. (1987) *Eur. Biophys. J.* **14,** 131–138.
15. Greenblatt, R. A., Blatt, Y. & Montal, M. (1985) *FEBS Lett.* **193,** 125–134.
16. Guy, H. R. & Seetharamulu, P. (1986) *Proc. Natl. Acad. Sci. USA* **83,** 508–512.
17. Kosower, E. M. (1985) *FEBS Lett.* **182,** 234–242.
18. Finer-Moore, J. & Stroud, R. M. (1984) *Proc. Natl. Acad. Sci. USA* **81,** 155–159.
19. Imoto, K., Methfessel, C., Sakmann, B., Mishina, M., Mori, Y., Konno, T., Fukuda, K., Kurasaki, M., Bujo, H., Fujita, Y. & Numa, S. (1986) *Nature (London)* **324,** 670–674.
20. Mishina, M., Tobimatsu, T., Imoto, K., Tanaka, K., Fujita, Y., Fukuda, K., Kurasaki, M., Takahashi, H., Morimoto, Y., Hirose, T., Inayama, S., Takahashi, T., Kuno, M. & Numa, S. (1985) *Nature (London)* **313,** 364–369.
21. Barany, G. & Merrifield, R. B. (1980) in *The Peptides: Analysis, Synthesis, Biology,* eds. Gross, E. & Meienhofer, J. (Academic, New York), Vol. 2, pp. 1–255.
22. Suarez-Isla, B. A., Wan, K., Lindstrom, J. & Montal, M. (1983) *Biochemistry* **22,** 2319–2323.
23. Oiki, S., Danho, W. & Montal, M. (1987) *Soc. Neurosci.* **13,** 576 (abstr.).
24. Tam, J. P., Heath, W. F. & Merrifield, R. B. (1983) *J. Am. Chem. Soc.* **105,** 6442–6455.
25. Montal, M., Anholt, R. & Labarca, P. (1986) in *Ion Channel Reconstitution,* ed. Miller, C. (Plenum, New York), pp. 157–204.
26. Cota, G. & Armstrong, C. M. (1987) *Biophys. J.* **51,** 49 (abstr.).
27. Labarca, P., Lindstrom, J. & Montal, M. (1984) *J. Gen. Physiol.* **83,** 473–496.
28. Labarca, P., Rice, J. A., Fredkin, D. R. & Montal, M. (1985) *Biophys. J.* **47,** 469–478.
29. Bezanilla, F. (1985) *Biophys. J.* **47,** 437–441.
30. Garnier, J., Osguthorpe, D. J. & Robson, B. (1978) *J. Mol. Biol.* **120,** 97–120.
31. Chou, P. Y. & Fasman, G. D. (1978) *Adv. Enzymol.* **47,** 45–148.
32. Schiffer, M. & Edmunson, A. B. (1967) *Biophys. J.* **7,** 121–135.
33. Blaurock, A. E. & Wilkins, M. H. F. (1969) *Nature (London)* **223,** 906–909.
34. Eisenberg, D., Schwarz, E., Komaromy, M. & Wall, R. (1984) *J. Mol. Biol.* **179,** 125–143.
35. Brooks, B. R., Bruccoleri, R. E., Olafson, B. D., States, D. J., Swaminathan, S. & Karplus, M. (1983) *J. Comp. Chem.* **4,** 187–217.